Progress In Electromagnetics Research M, Vol. 82, 167–173, 2019

Defect Mode Tuning in Two-Dimensional Band-Gap Wire Structure in the Millimeter Waveband

Liubov I. Ivzhenko[1, *], Eugene N. Odarenko[2], Daria I. Yudina[3], and Segey I. Tarapov[1, 2, 3]

Abstract—A two-dimensional (2D) band-gap wire structure with a spatial defect has been fabricated and studied in order to demonstrate which way the violation of periodicity affects its spectral properties. We experimentally demonstrate and numerically verify the occurrence of defect modes revealed as localized resonant peak inside the band gap transmission spectrum of 2D band-gap wire structure. We also demonstrate the efficient frequency tunability of these defect mode peaks by varying defect size in the frequency range 22–40 GHz. The visualization and analysis of spatial electromagnetic (EM) field distribution within the defect of 2D band-gap wire structure is performed both experimentally and numerically. A good agreement between the experiment and numerical simulation is demonstrated.

1. INTRODUCTION

The physical phenomenon commonly known as "defective state" or "defective mode" in photonic crystals (PCs) has attracted a great deal of interests due to their unique electromagnetic properties and potential applications in optoelectronics and optical communications [1–4]. It is known that the defect mode arises from the intentional introduction of a spatial defect into the PC structure [5]. Since in nature, the disordered structures occur more often [6, 7] than an ideal periodicity, this explains why investigations of these phenomena today are still of great importance for researchers. Modes of this type lead to high localization of electromagnetic (EM) field in both frequency and spatial domains. So, defect modes can be successfully applied to the design of various types of frequency and spatial filters [8, 9] with ability to control their parameters in a wide frequency range from GHz to optical one. Localized electromagnetic waves with frequencies arising in the middle of the band gap due to the spatial defect in the periodic structure have been studied for instant in [8–11]. Also, there are a large number of papers devoted to this phenomenon where the frequency of this defect mode is adjusted by applying static magnetic field [11, 12]. In addition, the combination of periodic band gap structures with such type of structures as graphene or chiral elements has been considered extensively [10, 13].

A large number of investigations have been performed for one- and two-dimensional photonic crystals with similar phenomena, so called Tamm state, which are not directly relevant to our work.

In our case, we consider the microwave analog of PC (2D wire mesh photonic crystal [5, 15]) formed by the periodic wire array with rectangular unit cell [14, 15]. It is necessary to note that such metamaterial could be attributed also to plasma-like medium, under conditions when wire size and periods are much smaller than the wavelength [16, 17].

The precise definition of the region in space, where the defect modes is located, is essential to many applications where the electromagnetic field should be confined in some specific volume. Despite

Received 4 February 2019, Accepted 21 June 2019, Scheduled 4 July 2019

* Corresponding author: Liubov I. Ivzhenko (ivzhenko@ire.kharkov.ua).

[1] Radiospectroscopy Department, O.Ya. Usikov Institute for Radiophysics and Electronics of NASU, 12, Ak. Proskura Str., Kharkiv 61085, Ukraine. [2] Kharkiv National University of Radio Electronics, 14, Nauka Ave., Kharkiv 61166, Ukraine. [3] Karazin Kharkiv National University, 4, Svobody Sq., Kharkiv 61022, Ukraine.

significant research efforts, there is still a lack of sufficient number of new and mainly effective methods of accurate registration of the EM field distribution within metamaterials.

In this paper, we suggest a simple experimental method to detect and analyze the spatial field distribution inside 2D finite-size wire structure with spatial defect in the millimeter waveband. Our numerical modeling performed in MEEP package, showing high computational efficiency and high convergence, is competitive compared to other widespread commercial FDTD-packages.

2. EXPERIMENTAL INVESTIGATION OF TWO-DIMENSIONAL BAND-GAP WIRE STRUCTURE WITH SPATIAL DEFECT

We develop and fabricate a two-dimensional (2D) wire medium metamaterial formed by a periodic array of thin copper wires (see Fig. 1(a)).

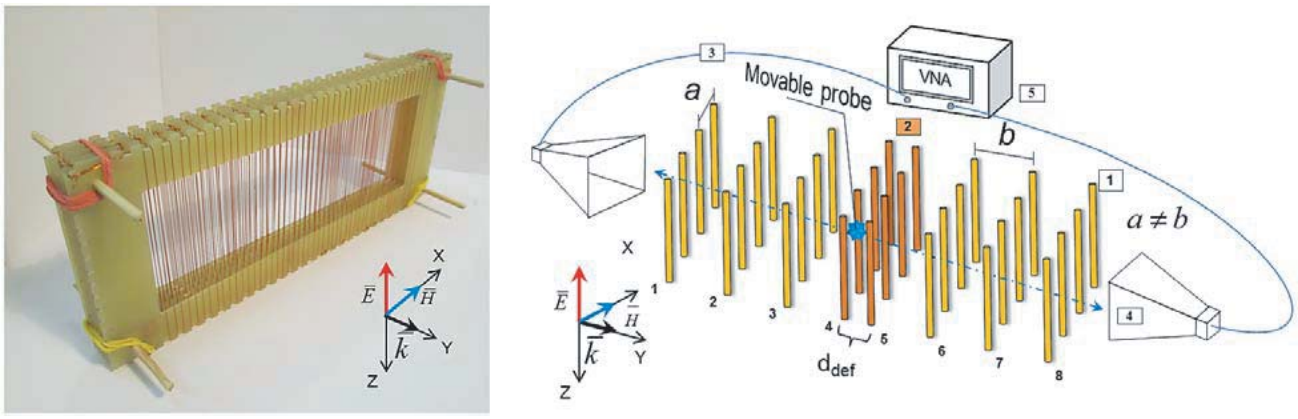

(a) (b)

Figure 1. (a) The photo of 2D photonic bandgap wire structure; (b) the scheme of experimental installation for registration of the EM field distribution using test body method within 2D wire medium structure (1) with defect (2), where 3 — coaxial cables; 4 — transmitting and receiving horn antennas; 5 — VNA.

The description of the wire structure is defined by the parameters: a — period along the x axis, b — period along the y axis, N — number of wire rows, d_{def} — defect thickness, which is represented as the spacing between the centers of the wires in rows 4 and 5. The wires 0.315 mm in diameter are located periodically in Ox and Oy directions with the periods ($a \neq b$). Thus, the unit cell of such PC has the form of a rectangle in XOY plane. Wires located with a period a along the x-axis form several ($N = 8$) rows with number N, as illustrated in Fig. 1(b). Copper wires are fixed on a fiberglass frame with thickness 1.5 mm and period $a = 3$ mm. Frames (in all 8 pcs.) of identical thickness are fixed in succession one after the other along the y axis at a distance $b = 6.5$ mm. Thus, we use the row-by-row photonic crystal based on rectangle shaped copper wires, with violation of periodicity in the center of the structure. In the cases studied, the wave vector **k** is directed along the y axis (see Fig. 1(b)). The period b is approximately equal to one-half the length of a wavelength ($b \cong \lambda/2$), so that the frequency spectrum acquires a bandgap characteristic. In general, the spatial defect is presented as a deviation from b-period size, i.e., in the cases reviewed $d_{def} < b$ and $d_{def} > b$. d_{def} represents the spacing between the centers of the neighbor wires in rows 4 and 5 in the direction of the y-axis.

Firstly, the transmission spectra of 2D band-gap wire structure were obtained experimentally. The empirical studies were carried out in the operating frequency range 22–40 GHz. Measurements of the transmission coefficient are performed under normal incidence conditions for the case, when **E** vector directed along the wires (TE-polarization). The wire structure is located between the broadband horns, which are the source and receiver of electromagnetic waves with a nearly plane wave front. Vector Network Analyzer (N5230A) is used for analysis of the phenomena under study.

The typical spectral curves of the transmittance for the case of the wire structure with a spatial defect are presented in Fig. 2.

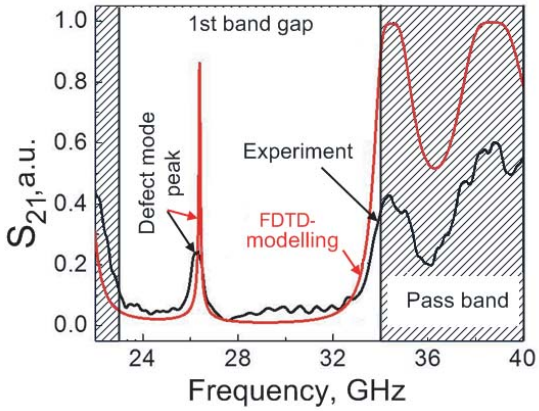

Figure 2. Transmission spectra of 2D PBG wire structure with spatial defect (d_{def} = 4.5 mm): experiment (black color line), FDTD simulation (red color line).

The wire structure exhibits the 1st band gap for TE-polarized modes extending from 24 to 34 GHz. The 1st bandgap is clearly visible at the transmission spectra and limited by the frequency passbands marked with hatching. This phenomenon is described in detail in [15]. As can be seen form Fig. 2, the introduction of the defect into the wire structure results in appearance of a narrow transmission peak in the 1st band gap. Results of measurements (black curve) and numerical calculations (red curve) are presented here. These two peaks are coincident well.

Secondly, in order to detect the EM field distribution inside above-mentioned wire structure, we used the test body method [18] in our experiment for theoretical revising. This method is well applicable to recording and analyzing the spatial distribution of the EM field. According to [14], the amplitude distribution of the EM field is recorded by changing the transmission spectra, when a probe is introduced into the required part of the space within the wire structure [19]. To detect the spatial field distribution, we applied a well-known perturbation technique. The probe moves inside the structure along a given trajectory by the scanner [19] and the controlled program.

The steel sphere with a diameter of 1.56 mm was used as a probe. The size of the sphere was chosen empirically based on the most complete picture of the amplitude field distribution in the vicinity of the spatial defect. Thus, a one-dimensional scanning of the EM field was provided along the entire structure.

3. THE SPECTRAL AND DISPERSIVE PROPERTIES OF TWO-DIMENSIONAL BAND-GAP WIRE STRUCTURE WITH SPATIAL DEFECT

The spectral and dispersive properties of the 2D band-gap wire structure are investigated by numerical simulation with the finite difference time domain (FDTD) method, using a freely available software package MEEP [20].

In our numerical model we consider a 2D row-by-row wire structure with a spatial defect, which is shown in Fig. 3(a); such a structure can support the propagation of TE-modes. All wires are made from copper. The thickness of the wire structure is described by expression: $L = 3b + d_{def} + 3b$. Simulations were performed with small grid step to assure the accuracy of the calculations results. Resolution parameter value corresponds to 32 pixels per distance unit (1 mm). Further, we suppose that the structure is illuminated by a normally incident plane wave along y-axis with its electric field polarized along the wires (TE-polarization).

To simulate the dispersive properties of the wire structure, the unit cell ideology is used. The form of the unit cell is chosen to be a row of wires with periodicity violation (Fig. 3(b)); therefore, each unit cell is symmetric about the line drawn through the cell center parallel to the x-axis. In fact, we consider

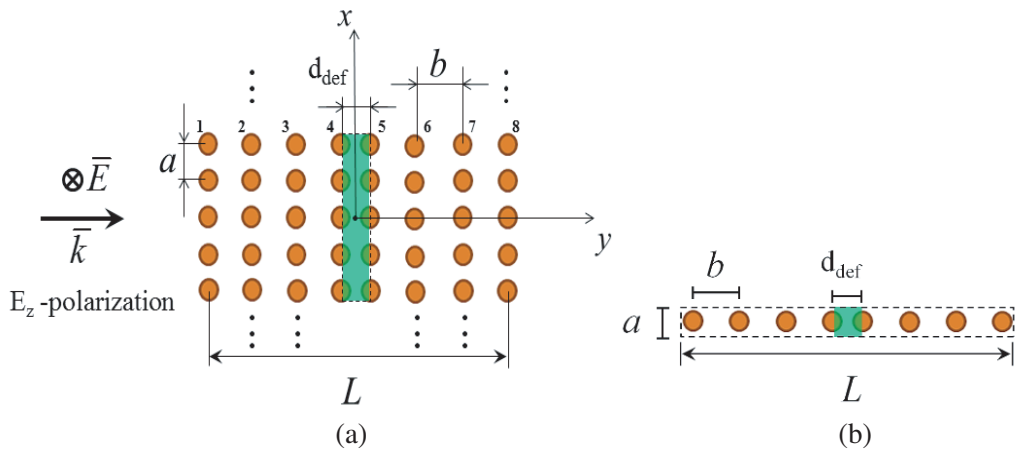

Figure 3. (a) 2D band-gap wire structure with a spatial defect that used in MEEP — modeling: a, b — structure periods, d_{def} — defect thickness, L — wire structure length; (b) unit cell geometry.

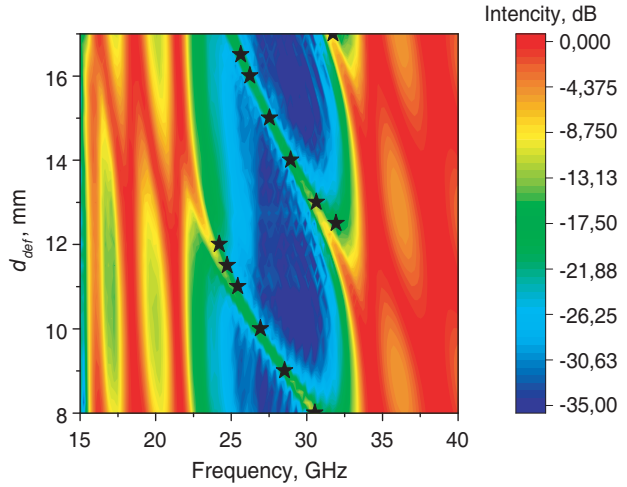

Figure 4. 2D transmission spectrum of 2D wire structure with defect (d_{def}): black asterisks — experiment.

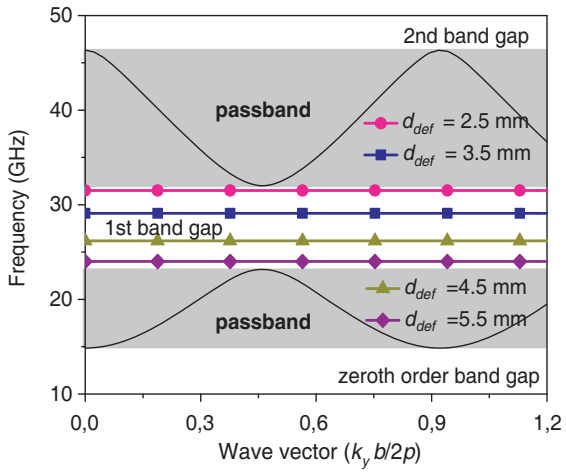

Figure 5. Evolution of dispersion curves corresponding to defect mode of the 2D band-gap wire structure with changing defect size d_{def} value.

periodical structure in y-direction. It is apparent that physically valid results we obtain physically valid results only in the case when field coupling between periodicity defects can be neglected. Exactly this mode is realized in the wire medium when we simulate resonance regime that corresponds to "defect" mode.

In order to demonstrate how the thickness of defect layer influences the spectral characteristics of the structure under study, we plotted numerical and experimental spectra, which demonstrate the frequency dependence of the defect mode peak. Fig. 4 shows 2D transmission spectrum of wire structure with a spatial defect for various d_{def} obtained by numerical calculations. Also, the frequency of defect mode peaks obtained experimentally is denoted by black asterisks. As can be seen from Fig. 4, a good agreement between the experiment and numerical calculations is demonstrated.

In the wire structure, TE modes propagate along the OY-axis (15–23 GHz) under the conditions $\lambda/b = 3$ as shown in [14]. Above this value, part of the wave will be reflected, i.e., a stationary wave is formed. The half wavelength for one of the geometric dimensions $b = 6.5$ mm is stacked along the period. Thus, such a structure will form the 1st band gap (23–34 GHz) due to Bragg scattering (Fig. 4).

It is clear that with increasing the d_{def} parameter from $d_{def} \geq 8$ mm to a certain critical value of $d_{def} \leq 12$ mm (with step 0.5 mm) the frequency of transmission peak monotonically decreases from

33 GHz to 24 GHz. It is easy to see that defect mode peak disappears at the boundary of the passband with a further increase of the cavity thickness. However, starting with $d_{def} \geq 12.5$ mm, we can observe the 2nd transmission peak at the frequency of 31.6 GHz inside the 1st band gap.

This second peak shifts, also, with a further increase in the thickness of the defect layer to the low frequency range. The 2nd peak vanished when the thickness $d \geq 16.5$ mm was reached (as for the thickness of $d_{def} \geq 12$ mm). This peak enters into the passband. Further, the 3rd peak appears in high-frequency area of band gap with further increase $d_{def} \geq 16$ mm (placed inside the wire structure). The legend is repeated. Thus the resonance peak wavelength increases proportionally to d. It is obvious that the 1st, 2nd, and 3rd peaks correspond to the fact that approximately 2, 3, and 4 half-waves fit in the defect layer responsible for their formation. Note that these dispersion characteristics fully correspond to the presentation described in [6, 7, 14, 15].

Figure 5 shows a dispersion diagram along the wave propagation direction with the zeroth order and first order TE propagating modes of the infinite 2D band-gap wire medium with symmetry that corresponds to Fig. 3.

Here, we represent frequencies without any normalization for better ability of comparison with experimental data. But wave vector is normalized in a usual manner for dispersion diagrams of the periodical structures. Earlier, in [14] it was shown that periods of wires' location at the medium describe the characteristic shape of dispersive curves, marked in Fig. 5 with black color. The parameter a determines the width of passbands, namely, the width of band gaps increases with period a decreasing. Primary 2D band-gap wire structure in the low-frequency region of microwaves possesses electromagnetic properties that correspond to a homogeneous plasma-like medium at $\lambda/b > 3$. Consequently, we observe zeroth-order band gap (0–15 GHz) restricted by dispersive curve that corresponds to $a = 3$ mm, $b = 6.5$ mm. At the same time, for a high-frequency region, when the wavelength is comparable with period b, the wire structure acquires properties of a photonic crystal with zone characteristic of transmission spectra. As a result, we observe the 1st band gap (23–32 GHz) and 2nd band gap at $f \geq 46$ GHz. As can be seen in Fig. 5, with adding a spatial defect into the structure, we observe in the 1st band gap the appearance of a defect mode, which is marked as a straight line with dots. As for spectra we can observe that the defect mode shifts to the low-frequency region with parameter d_{def} increasing.

4. VISUALIZATION AND ANALYSIS OF SPATIAL FIELD DISTRIBUTION IN WIRE STRUCTURE

In order to analyze the resonant nature of the transmission, we obtained experimentally and numerically the spatial distribution of EM-field relating to defect mode. Fig. 6 shows that the red curve is an experiment, and the black curve is theory.

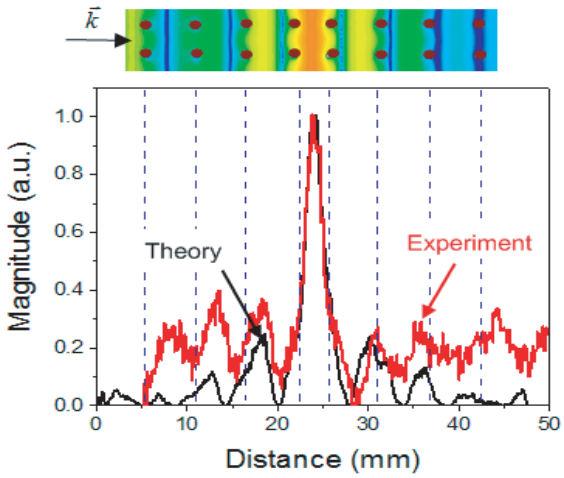

Figure 6. The experimental and numerical distribution of the defect mode field in the 2D wire structure ($N = 4$) with the spatial defect ($d_{def} = 4$ mm) at $f = 30.09$ GHz.

Previously, it was mentioned that a narrow transmission peak within the band gap spectrum was observed with d_{def} increasing, namely with a value of $\lambda/3$ approximately. As a result, the concentration of EM-field within the limits of defect thickness is formed. This concentration corresponds to a resonance oscillation represented by standing wave. Recall that the defect size (responsible for the formation of defect modes) is not a multiple of the wavelength at a given frequency, but smaller that this value. We observe a change in the intensity of the electric field, at a time as the probe moves within the scanning region of the structure. Data related to field intensity changing at the chosen frequency are recorded and processed by the VNA. As can be seen from Fig. 6, the electric field is concentrated within the region of the defect itself. Therefore, the magnitude of electric field component steadily decreases when it is moves away from the defect vicinity, as shown in the insert of Fig. 6. Fig. 6 shows a good coincidence between the experimental data and the data obtained by numerical calculations.

5. CONCLUSION

We used the test body method to detect and analyze the spatial field distribution inside a 2D finite-size wire structure with spatial defect in the millimeter waveband.

Thus, 2D band-gap wire structure with a spatial defect has been fabricated and studied. We demonstrated experimentally and verified numerically the occurrence of defect modes that reveal itself as localized resonant peak. We also demonstrated the frequency tunability of these defect mode peaks by varying defect size in the frequency range 22–40 GHz. The experimental and numerical visualization and analysis of the spatial EM field distribution in the defect of the 2D band-gap wire structure are performed. A good coincidence between the experiment and numerical simulation is demonstrated.

We expect that the novel type of metamaterial studied here should find applications as electronically controlled elements of GHz and THz band devices (isolators, signal modulators, high-sensitive sensors, etc.).

REFERENCES

1. Ozbay, E. and M. Bayindir, "Physics and applications of defect structures in photonic crystals," A. S. Shumovsky, V. I. Rupasov, (eds.), "Quantum communication and information technologies," *NATO Science Series (Series II: Mathematics, Physics and Chemistry)*, Vol. 113, Springer, 2003, *Philos. Mag.*, Vol. 14, 60–65, 1907.
2. Noda, S., M. Fujita, and T. Asano, "Spontaneous-emission control by photonic crystals and nanocavities," *Nat. Photonics*, Vol. 1, 449–458, 2007.
3. Ma, G., J. Shen, Z. Zhang, Z. Hua, and S. H. Tang, "Ultrafast all-optical switching in one-dimensional photonic crystal with two defects," *Opt. Express*, Vol. 14, 858–865, 2006.
4. Painter, O., J. Vučković, and A. Scherer, "Defect modes of a two-dimensional photonic crystal in an optically thin dielectric slab," *J. Opt. Soc. Am. B*, Vol. 16, No. 2, 1999.
5. Sievenpiper, D. F., M. E. Sickmiller, and E. Yablonovitch, "3D wire mesh photonic crystals," *Phys. Rev. B*, Vol. 76, No. 14, 2480–2483, 1996.
6. Pierre, C., "Weak and strong vibration localization in disordered structures: A statistical investigation," *Journal of Sound and Vibration*, Vol. 139, 111–132, 1990.
7. Ziegler, F., "Wave propagation in periodic and disordered layered composite elastic materials," *International Journal of Solids and Structures*, Vol. 13, 293–305, 1977.
8. Munday, J. N. and W. M. Robertson, "Slow electromagnetic pulse propagation through a narrow transmission band in a coaxial photonic crystal," *Appl. Phys. Lett.*, Vol. 83, 1053, 2003.
9. Chen, C.-P., T. Anada, S. Greedy, T. M. Benson, and P. Sewell, "A novel photonic crystal band-pass filter using degenerate modes of a point-defect microcavity for terahertz communication systems," *Microwave and Optical Technology Letters*, Vol. 56, 792–797, 2014.
10. Fan, H.-M., T.-B. Wang, N.-H. Liu, J.-T. Liu, Q.-H. Liao, and T.-B. Yu, "Tunable plasmonic band gap and defect mode in one-dimensional photonic crystal covered with graphene," *J. Opt.*, Vol. 16, 125005, 2014.

11. Hamidi, S. M., M. M. Tehranchi, and M. Shasti, "Engineered one-dimensional magneto-photonic crystals for wavelength division multiplexing systems," *J. Phys. D: Appl. Phys.*, Vol. 44, 205107, 2011.
12. Kharchenko, A. A. and S. I. Tarapov, "The spectrum of one-dimensional magnetophotonic crystal in the vicinity of the ferromagnetic resonance: Magnetic field dependence," *Telecommunications and Radio Engineering*, Vol. 72, No. 20, 1865–1872, 2013.
13. Lee, K. J., J. W. Wu, and K. Kim, "Defect modes in a one-dimensional photonic crystal with a chiral defect layer," *Optical Materials Express*, Vol. 4, No. 12, 2542–2550, 2014.
14. Ivzhenko, L. I., E. N. Odarenko, and S. I. Tarapov, "Mechanically tunable wire medium metamaterial in the millimeter wave band," *Progress In Electromagnetics Research Letters*, Vol. 64, 93–98, 2016.
15. Ivzhenko, L. I., D. I. Yudina, and S. I. Tarapov, "Defective modes in an anisotropic wire metamaterial in the microwave range," *Telecommunications and Radio Engineering*, Vol. 76, No. 19, 1681–1688, 2017.
16. Rotman, W., "Plasma simulation by artificial and parallel plate media," *IRE Trans. Ant. Propagat.*, Vol. 10, No. 1, 82–95, 1962.
17. Pendry, J. B., A. J. Holden, W. J. Stewart, et al., "Extremely low frequency plasmons in metallic mesostructures," *Phys. Rev. Lett.*, Vol. 76, No. 25, 4773–4776, 1996.
18. Valitov, R. A., S. F. Dyubko, V. V. Kamyshan, and V. P. Sheiko, "Method for measuring the field distribution in an open reson," *Soviet Physics — JETP*, Vol. 20, No. 4, 791–1077, 1965.
19. Kozhara, L. I., S. Y. Polevoy, and I. V. Popov, "Technique for analysis of the spatial field distribution in tapered wire medium," *Solid State Phenomena*, Vol. 214, 75–82, 2014.
20. Oskooi, A. F., D. Roundy, M. Ibanescu, P. Bermel, J. Joannopoulos, and S. G. Johnson, "MEEP: A flexible free-software package for electromagnetic simulations by the FDTD method," *Computer Physics Communications*, Vol. 181, 687–702, 2010.